

Bayesian Self-Supervised Contrastive Learning

Bin Liu¹ Bang Wang^{*1}

Abstract

Recent years have witnessed many successful applications of contrastive learning in diverse domains, yet its self-supervised version still remains many exciting challenges. As the negative samples are drawn from unlabeled datasets, a randomly selected sample may be actually a false negative to an anchor, leading to incorrect encoder training. This paper proposes a new self-supervised contrastive loss called the BCL loss that still uses random samples from the unlabeled data while correcting the resulting bias with importance weights. The key idea is to design the desired sampling distribution for sampling hard true negative samples under the Bayesian framework. The prominent advantage lies in that the desired sampling distribution is a parametric structure, with a location parameter for debiasing false negative and concentration parameter for mining hard negative, respectively. Experiments validate the effectiveness and superiority of the BCL loss¹.

1. Introduction and Contribution

Unsupervised learning has been extensively researched for its advantages of learning representations without human labelers for manually labeling data. How to learn good representation without supervision, however, has been a long-standing problem in machine learning. Recently, *contrastive learning* that leverages a *contrastive loss* (Chopra et al., 2005; Hadsell et al., 2006) to train a representation encoder has been promoted as a promising solution to this problem (Oord et al., 2018; Tian et al., 2020; Liu et al., 2021; Chen et al., 2020b). Remarkable successes of contrastive learning have been observed for many applications in different domains (Alec et al., 2018; 2019; Misra & Maaten, 2020; He et al., 2020). Nonetheless, its potentials can be further released for a better contrastive loss being designed.

We study the following *self-supervised contrastive learning* problem (Oord et al., 2018; Chuang et al., 2020; Robin-

son et al., 2021; Chen et al., 2020a; Chuang et al., 2020; Liu et al., 2021): Consider an unlabeled dataset \mathcal{X} and a class label set \mathcal{C} , let $h : \mathcal{X} \rightarrow \mathcal{C}$ be the classification function assigning a *data point* $x \in \mathcal{X}$ with a *class label* $c \in \mathcal{C}$. Assume that observing a class label $\rho(c) = \tau^+$ is uniform and $\tau^- = 1 - \tau^+$ is the probability of observing any different class. For a given data point x , let $p^+(x^+) = p(x^+ | h(x) = h(x^+))$ denote the probability of another point x^+ with the same label as x , and in such a case, x^+ is called a *positive sample* specific to x . Likewise, let $p^-(x^-) = p(x^- | h(x) \neq h(x^-))$ denote the probability of another point x^- with a different label to x , and in such a case, x^- is called a *negative sample* specific to x . Let $f : \mathcal{X} \rightarrow \mathbb{R}^d$ denote the representation learning function (i.e., encoder) to map a point x to an *embedding* $f(x)$ on a d -dimensional hypersphere.

Self-supervised contrastive learning is to contrast similar pairs (x, x^+) and dissimilar pairs (x, x^-) to learn the encoder f (Wang & Isola, 2020; Wang & Liu, 2021; Chuang et al., 2020); While the objective is to encourage representations of (x, x^+) to be closer than that of (x, x^-) . In training the encoder, we randomly draw a point from the underlying data distribution p_d on \mathcal{X} , i.e., $x \sim p_d$, and its positive sample x^+ can be easily obtained from some semantic-invariant operation on x like image masking, written as $x^+ \sim p^+$. In practice, a negative sample x^- is drawn from the unlabeled dataset and $x^- \sim p_d$. However, the sample x^- could be potentially with the same label as x , i.e., it is a *false negative* to x . In such a case, the construction of a dissimilar pair (x, x^-) would degrade the learned representations (Wang & Liu, 2021; Chuang et al., 2020). As no prior knowledge about the label of x^- , we propose to include an *importance weight* ω to measure the credibility of a constructed pair (x, x^-) for contrastive learning.

Contribution: In this paper, we propose the following Bayesian self-supervised Contrastive Learning objective function, viz., the BCL loss:

$$\mathcal{L}_{\text{BCL}} = \mathbb{E}_{\substack{x \sim p_d \\ x^+ \sim p^+ \\ x^- \sim p_d}} -\log \left[\frac{e^{f(x)^T f(x^+)}}{e^{f(x)^T f(x^+)} + \sum_{i=1}^N \omega_i \cdot e^{f(x)^T f(x_i^-)}} \right],$$

Our main contributions include (i) the derivation of parametric structural sampling distribution conditioned on *hard principle* and *true principle*, (ii) the posterior estimation

¹liubin0606@hust.edu.cn; wangbang@hust.edu.cn; School of Electronic Information and Communications, Huazhong University of Science and Technology (HUST), Wuhan, China. Corresponding author: Bang Wang

of a unlabeled sample being true negative sample, and (iii) the stochastic process depiction to simulate predictions of neural networks.

Compared with the InfoNCE (Oord et al., 2018), we include the importance weight ω in the contrastive loss, which is designed to down-weight a constructed pair (x, x^-) for x^- being a false negative sample or to up-weight (x, x^-) for x^- being a true negative sample. The key idea is to design a desired sampling distribution for hard true negative samples under the Bayesian framework. The prominent advantage lies in that we derive the parametric structure for the desired sampling distribution with a location parameter for debiasing false negative and concentration parameter for mining hard negative, respectively. More detailed analysis on \mathcal{L}_{BCL} and derivation of ω computation are given in the subsequent sections.

We summarize the computation of ω in each training epoch as follows. In a training epoch, we randomly draw N samples $\{x_i^-\}_{i=1}^N$ from training set, which are assumed as negative samples specific to x . Let $\hat{x}_i^- = \exp(f(x)^T f(x_i^-))$ denote the power exponent of similarity between x and x_i^- . We compute the importance weight ω_i for x_i^- by the following three steps:

Step-1: Compute $\Phi_N(\hat{x}_i^-)$, called the empirical distribution function of \hat{x}_i^- ,

$$\Phi_N(\hat{x}_i^-) = \frac{1}{N} \sum_{j=1}^N \mathbb{I}(\hat{x}_j^- \leq \hat{x}_i^-), \quad (1)$$

where $\mathbb{I}(\cdot)$ is the indicator function.

Step-2: Compute $p(\text{TN}|\hat{x}_i^-)$, the posterior probability of x_i^- being a true negative (TN) to x ,

$$p(\text{TN}|\hat{x}_i^-) = \frac{\alpha\tau^- + (1-2\alpha)\Phi_N(\hat{x}_i^-)\tau^-}{\alpha\tau^- + (1-\alpha)\tau^+ + (1-2\alpha)\Phi_N(\hat{x}_i^-)(\tau^- - \tau^+)}, \quad (2)$$

where α is a hyperparameter to be explained latter.

Step-3: Compute $\omega_i(\hat{x}_i^-)$, the importance weight of x_i^- for correcting the bias between actual sampling distribution and desired sampling distribution

$$\omega_i(\hat{x}_i^-) = \frac{p(\text{TN}|\hat{x}_i^-) \cdot \hat{x}_i^\beta}{\frac{1}{N} \sum_{i=1}^N p(\text{TN}|\hat{x}_i^-) \cdot \hat{x}_i^\beta}, \quad (3)$$

where β is a hyperparameter to be explained latter.

2. Contrastive Loss and Analysis

2.1. Contrastive Loss

In the context of *supervised contrastive learning*, dissimilar pairs (x, x^-) can be easily constructed by randomly drawing a true negative sample x^- specific to x , i.e., $x^- \sim p^-$,

based on the sample label. The *contrastive predictive coding* (CPC) (Oord et al., 2018) introduces the following InfoNCE loss (Gutmann & Hyvärinen, 2010; 2012):

$$\mathcal{L}_{\text{SUP}} = \mathbb{E}_{\substack{x \sim p_d \\ x^+ \sim p^+ \\ x^- \sim p^-}} \left[-\log \frac{e^{f(x)^T f(x^+)}}{e^{f(x)^T f(x^+)} + \sum_{i=1}^N e^{f(x)^T f(x_i^-)}} \right] \quad (4)$$

to learn an encoder $f: \mathcal{X} \rightarrow \mathbb{R}^d/t$ that maps a data point x to the hypersphere \mathbb{R}^d of radius $1/t$, where t is the temperature scaling. As in the CPC, we also set $t = 1$ in our theoretical analysis.

In the context of *self-supervised contrastive learning*, however, as samples' labels are not available, i.e., $p^-(x') = p(x'|h(x) \neq h(x'))$ is not accessible, the standard approach is to draw N samples from the data distribution p_d , which are supposed to be negative samples to x , to optimize the following InfoNCE *self-supervised contrastive loss*:

$$\mathcal{L}_{\text{BIASED}} = \mathbb{E}_{\substack{x \sim p_d \\ x^+ \sim p^+ \\ x^- \sim p_d}} \left[-\log \frac{e^{f(x)^T f(x^+)}}{e^{f(x)^T f(x^+)} + \sum_{i=1}^N e^{f(x)^T f(x_i^-)}} \right]. \quad (5)$$

Following the DCL (Chuang et al., 2020), it is also called as *biased contrastive loss* since those supposedly negative samples x^- drawn from p_d might come from the same class as the data point x with probability τ^+ .

2.2. Sampling Bias Analysis

Let $x^- \in \text{TN}$ denote x^- being a *true negative* (TN) sample specific to x . Let $x^- \in \text{FN}$ denote x^- being a *false negative* (FN) sample specific to x , i.e. x^- and x are with the same ground truth class label. Note that whether x^- is a TN or FN is specific to a particular *anchor* point x , and in what follows, we omit the *specific to x* for brevity. It has been proven that for $\{x_i^- \in \text{TN}\}_{i=1}^N$, optimizing the InfoNCE loss \mathcal{L}_{SUP} will result in the learning model estimating and optimizing the *density ratio* $\frac{p^+}{p^-}$ (Oord et al., 2018; Poole et al., 2019). Denote $\hat{x}^+ = e^{f(x)^T f(x^+)}$. The CPC (Oord et al., 2018) proves that minimizing \mathcal{L}_{SUP} leads to

$$\hat{x}^+ \propto p^+/p^-. \quad (6)$$

As discussed by (Oord et al., 2018), p^+/p^- preserves the mutual information (MI) of future information and present signals, where MI maximization is a fundamental problem in science and engineering (Poole et al., 2019; Belghazi et al., 2018).

Now consider the InfoNCE loss $\mathcal{L}_{\text{BIASED}}$, which can be regarded as the categorical cross-entropy of classifying one positive sample x^+ from unlabeled samples. For analysis purpose, we rewrite x^+ as x_0 . Given $N+1$ unlabeled data points, the posterior probability of one data point x_0 being

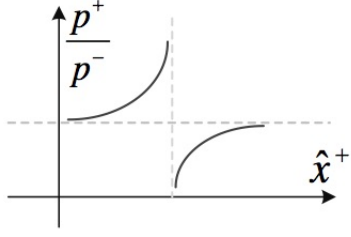


Figure 1. Illustration of $\mathcal{L}_{\text{BIASED}}$ and mutual information optimization by Eq. (10).

a positive sample can be derived by

$$\begin{aligned} & P(x_0 \in \text{pos} | \{x_i\}_{i=0}^N) \\ &= \frac{p^+(x_0) \prod_{i=1}^N p_d(x_i)}{\sum_{j=0}^N p^+(x_j) \prod_{i \neq j} p_d(x_i)} \\ &= \frac{p^+(x_0)/p_d(x_0)}{p^+(x_0)/p_d(x_0) + \sum_{j=1}^N p^+(x_j)/p_d(x_j)} \end{aligned} \quad (7)$$

To minimize $\mathcal{L}_{\text{BIASED}}$, the optimal value for this posterior probability is 1, which is achieved in the limit of $p^+(x_0)/p_d(x_0) \rightarrow +\infty$ or $p^+(x_j)/p_d(x_j) \rightarrow 0$. Minimizing $\mathcal{L}_{\text{BIASED}}$ leads to

$$\hat{x}^+ \propto p^+/p_d. \quad (8)$$

Note that this is different from Eq. (6), since x_i^- may not be TN for lack of ground truth label.

Denote $\hat{x}^+ = m \cdot p^+/p_d$, $m \geq 0$. We investigate the gap between optimizing \hat{x}^+ and the optimization objective p^+/p^- . Inserting $p_d = p^- \tau^- + p^+ \tau^+$ back to Eq. (8), we obtain

$$\hat{x}^+ = m \cdot \frac{p^+}{p^- \tau^- + p^+ \tau^+}. \quad (9)$$

Rearranging the above equation yields

$$p^+/p^- = \frac{\hat{x}^+ \cdot \tau^-}{m - \hat{x}^+ \cdot \tau^+}. \quad (10)$$

Fig. 1 illustrates the approximate shape of Eq. (10) as a fractional function, which reveals the inconsistency between InfoNCE $\mathcal{L}_{\text{BIASED}}$ loss optimization and MI optimization. That is, when optimizing InfoNCE loss, the increase of \hat{x}^+ does not lead to the monotonic increase of p^+/p^- . Indeed, the existence of *jump discontinuity* indicates that the optimization of $\mathcal{L}_{\text{BIASED}}$ does not necessarily lead to the tractable MI optimization. The reason for the intractable MI optimization is from the fact that not all $\{x_i^-\}_{i=1}^N$ are TN samples, as

they are randomly drawn from the data distribution p_d . This leads to the inclusion of p^+ in the denominator of Eq. (9) when decomposing the data distribution p_d . Fig. 6 in Appendix provides an intuitive explanation. The four sampled data points actually contain one FN sample. Such a FN sample should be pulled closer to the anchor x . However, as it is mistakenly treated as a negative sample, during model training it will be pushed further apart from the anchor, which breaks the semantic structure of embeddings (Wang & Liu, 2021).

3. The Proposed Method

In this paper, we consider to randomly draw negative samples $\{x_i^-\}_{i=1}^N$ from the unlabeled dataset, i.e., $x_i^- \sim p_d$. As the class label is not accessible, x_i^- could be either a TN sample or a FN sample. We propose to include and compute an importance weight ω_i into the InfoNCE contrastive loss for correcting the resulting bias of drawing negative samples from p_d . The ideal situation is that we can set $\omega = 0$ to each FN sample, so that only the *hard true negative* samples contribute to the calculation of contrastive loss, which relies on the design of *desired sampling distribution*.

We consider the following two design principles of the *sampling distribution* for drawing $\{x_i^-\}_{i=1}^N$. The *true principle* (Wang & Liu, 2021; Robinson et al., 2021) states that the FN samples should not be pushed apart from the anchor x in the embedding space. The *hard principle* (Yannis et al., 2020; Robinson et al., 2021; Florian et al., 2015; Hyun et al., 2016) states that the *hard* TN samples should be pushed further apart in the embedding space.

3.1. False Negative Debiasing

We first consider the true principle for the design of sampling distribution. We denote the power exponent of similarity between an anchor x and another unlabeled sample x' as $\hat{x} = e^{f(x)^T f(x')}$. Assume that \hat{x} is independently and identically distributed with a *probability density function* ϕ and *cumulative distribution function* $\Phi(\hat{x}) = \int_{-\infty}^{\hat{x}} \phi(t) dt$. As x' can be either a TN sample or a FN sample, so ϕ contains two populations, denoted as ϕ_{TN} and ϕ_{FN} . The problem of computing the \mathcal{L}_{BCL} loss Eq. (1) is reduced to estimating the sum over $\hat{x} \sim \phi_{\text{TN}}$, i.e., $\sum_{i=1}^N e^{f(x)^T f(x_i^-)}$, while using samples $\hat{x} \sim \phi$.

Existing approaches for solving above problem is the density estimation to fit ϕ (Xia et al., 2022), where ϕ is parameterized as a two-component mixture of ϕ_{TN} and ϕ_{FN} , such as the Gaussian Mixture Model (Lindsay, 1995), Beta Mixture Model (Xia et al., 2022). To make the analysis possible, ϕ_{TN} and ϕ_{FN} are postulated to follow a simple density function with fixed parameters, which is a too strong assumption. In addition, the learning algorithm for estimating ϕ is expen-

sive, since the mixture coefficients that indicate the probability of $\hat{x} \in \text{TN}$ or FN are hidden variables. The parameters of ϕ_{TN} and ϕ_{FN} can only be obtained through the iterative numerical computation of the EM algorithm (Dempster et al., 1977) that are sensitive to initial values.

In this paper, we propose an analytic method without explicitly estimating ϕ , also called the nonparametric method in the statistical theory. Consider n random variables from ϕ arranged in the ascending order according to their realizations. We write them as $X_{(1)} \leq X_{(2)} \leq \dots \leq X_{(n)}$, and $X_{(k)}$ is called the k -th ($k = 1, \dots, n$) order statistics (David & Nagaraja, 2004). The probability density function (PDF) of $X_{(k)}$ is given by:

$$\phi_{(k)}(\hat{x}) = \frac{n!}{(k-1)!(n-k)!} \Phi^{k-1}(\hat{x}) \phi(\hat{x}) [1 - \Phi(\hat{x})]^{n-k}$$

By conditioning on $n = 2$ we obtain:

$$\phi_{(1)} = 2\phi(\hat{x})[1 - \Phi(\hat{x})] \quad (11)$$

$$\phi_{(2)} = 2\phi(\hat{x})\Phi(\hat{x}) \quad (12)$$

Next, we investigate the position of positive and negative samples on the hypersphere, so as to get a deep insight into ϕ_{TN} . Consider a (x, x^+, x^-) triple, there exists a closed ball $\mathfrak{B}[f(x), d^+] = \{f(\cdot) | d(f(x), f(\cdot)) \leq d^+\}$ with center $f(x)$ and radius d^+ , where $d^+ = \|f(x) - f(x^+)\|$ is the distance of anchor embedding $f(x)$ and positive sample embedding $f(x^+)$. Two possible cases arise: $f(x^-) \in \mathfrak{B}[f(x), d^+]$ or $f(x^-) \notin \mathfrak{B}[f(x), d^+]$, as illustrated by Fig. 2. We can describe the two cases with the Euclidean distance: Fig 2(a) corresponds to $d^+ < d^-$, and Fig 2(b) corresponds to $d^- \leq d^+$, where $d^- = \|f(x) - f(x^-)\|$. Note that the Euclidean distance $d^\pm = \sqrt{2/t^2 - 2f(x)^\top f(x^\pm)}$ since all embeddings $f(\cdot)$ are on the surface of a hypersphere of radius $1/t$, so we have $\hat{x}^- < \hat{x}^+$ for case (a), and $\hat{x}^+ \leq \hat{x}^-$ for case (b). Expressed in the notation of order statistics, \hat{x}^- (marked in blue in Fig 2) is a realization of $X_{(1)}$ for case (a), or \hat{x}^- is a realization of $X_{(2)}$ for case (b), respectively.

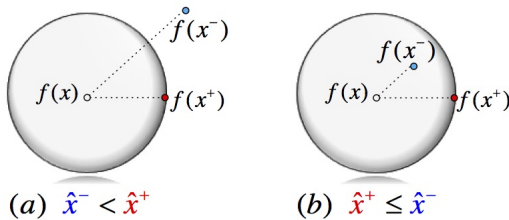


Figure 2. Two possible cases for the relative positions of anchor, positive, and negative triples.

The generation process of observation \hat{x} from ϕ_{TN} can be described as follows: Select case (a) with probability α , and

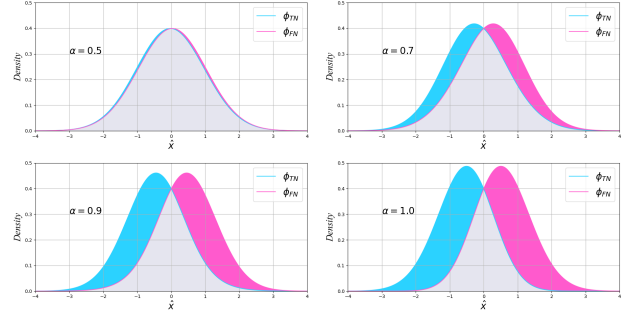


Figure 3. $\phi_{\text{TN}}(\hat{x})$ and $\phi_{\text{FN}}(\hat{x})$ with different α settings.

then generate an observation \hat{x} from $\phi_{(1)}$; Or select case (b) with probability $1 - \alpha$, and then generate an observation \hat{x} from $\phi_{(2)}$. That is, ϕ_{TN} is the component of $X_{(1)}$ and $X_{(2)}$ with a mixture coefficient α

$$\phi_{\text{TN}}(\hat{x}) = \alpha\phi_{(1)}(\hat{x}) + (1 - \alpha)\phi_{(2)}(\hat{x}) \quad (13)$$

Similarly, ϕ_{FN} is the component of $X_{(2)}$ and $X_{(1)}$ with mixture coefficient α :

$$\phi_{\text{FN}}(\hat{x}) = \alpha\phi_{(2)}(\hat{x}) + (1 - \alpha)\phi_{(1)}(\hat{x}) \quad (14)$$

Note that the way of taking \hat{x}^- as a realization of $X_{(1)}$ for case (a) omits the situation of $\hat{x}^- = \hat{x}^+$. The probability measure of \hat{x}^- for such case is 0 as ϕ is continuous density function dominated by Lebesgue measure.

Proposition 3.1 (Class Conditional Density). *If $\phi(\hat{x})$ is continuous density function that satisfy $\phi(\hat{x}) \geq 0$ and $\int_{-\infty}^{+\infty} \phi(\hat{x}) d\hat{x} = 1$, then $\phi_{\text{TN}}(\hat{x})$ and $\phi_{\text{FN}}(\hat{x})$ are probability density functions that satisfy $\phi_{\text{TN}}(\hat{x}) \geq 0$, $\phi_{\text{FN}}(\hat{x}) \geq 0$, and $\int_{-\infty}^{+\infty} \phi_{\text{TN}}(\hat{x}) d\hat{x} = 1$, $\int_{-\infty}^{+\infty} \phi_{\text{FN}}(\hat{x}) d\hat{x} = 1$.*

Proof. See Appendix C.1. \square

There may need a further understanding and clarification of the mixture coefficient α by reviewing Fig. 2. Intuitively, α is the probability that $f(x^-)$ falls out of $\mathfrak{B}[f(x), d^+]$. For a worst encoder f that randomly guesses, $\alpha = 0.5$; While for a perfect encoder $\alpha = 1$. Therefore, the reasonable value of $\alpha \in [0.5, 1]$. In fact, α reflects the encoder’s capability of scoring a positive sample higher than that of a negative sample, which admits the empirical macro-AUC metric over all anchors x in the training data set \mathcal{D} :

$$\begin{aligned} \alpha &= \int_{x \in \mathcal{X}} \int_0^{+\infty} \int_0^{+\infty} \mathbb{I}(\hat{x}^+ \geq \hat{x}^-) p(\hat{x}^+, \hat{x}^-) p(x) d\hat{x}^+ d\hat{x}^- dx \\ &\simeq \frac{1}{|\mathcal{D}|} \frac{1}{|\mathcal{D}^+| |\mathcal{D}^-|} \sum_{\mathcal{D}^+} \sum_{\mathcal{D}^-} \mathbb{I}(\hat{x}^+ \geq \hat{x}^-) \\ &= \frac{1}{|\mathcal{D}|} \text{AUC} \end{aligned} \quad (15)$$

By setting $\phi(\hat{x})$ as $\mathcal{N}(0, 1)$ in Eq. (11) and Eq. (12), we can get a quick snapshot of how α affects $\phi_{\text{TN}}(\hat{x})$ and $\phi_{\text{FN}}(\hat{x})$ as illustrated in Fig 3. The larger value of α results in higher discrimination of $\phi_{\text{TN}}(\hat{x})$ from $\phi_{\text{FN}}(\hat{x})$. This is also in accordance with our cognition that a better encoder encodes dissimilar data points with different class labels more orthogonal.

Based on the Bayes formula, the posterior probability of observing $\hat{x} \in \text{TN}$ is computed by

$$\begin{aligned} p(\text{TN}|\hat{x}) &= \frac{\phi_{\text{TN}}(\hat{x})\tau^-}{\phi_{\text{TN}}(\hat{x})\tau^- + \phi_{\text{FN}}(\hat{x})\tau^+} \end{aligned} \quad (16)$$

$$= \frac{\alpha\tau^- + (1 - 2\alpha)\Phi(\hat{x})\tau^-}{\alpha\tau^- + (1 - \alpha)\tau^+ + (1 - 2\alpha)\Phi(\hat{x})(\tau^- - \tau^+)} \quad (17)$$

$\phi(\hat{x})$ is eliminated due to the fractional form of the Bayesian formula. The posterior probability still belongs a nonparametric distribution family, since we do not know the specific expression of $\Phi(\hat{x}) = \int_{-\infty}^{\hat{x}} \phi(t)dt$. However, it converges to the following empirical distribution function

$$\Phi_n(\hat{x}) = \frac{1}{n} \sum_{i=1}^n \mathbb{I}_{|X_i| \leq \hat{x}}. \quad (18)$$

Glivenko theorem (Glivenko, 1933) has strengthened this result by proving the uniform convergence of $\Phi_n(\hat{x})$ to $\Phi(\hat{x})$. Note that $\Phi_n(\hat{x}) \in [0, 1]$ is the *sample information* in the Bayesian viewpoint, which includes a good probabilistic interpretation of the unlabeled data $x' \in \text{FN}$ given its observation \hat{x} . For a larger \hat{x} (with a closer embedding distance to the anchor), $\Phi_n(\hat{x})$ assigns a higher probabilistic prediction of the unlabeled sample x' sharing the identical latent class label with that of the anchor. In other words, $\Phi_n(\hat{x})$ can be regarded as the likelihood that reflects the explanation capability for the observation \hat{x} conditioning on the event of an unlabeled sample being a FN sample.

We note that $\Phi_n(\hat{x})$ allows us to obtain the analytical solution of the probability estimate $p(\text{TN}|\hat{x})$ from the non-parametric structural ϕ without postulation on ϕ . Also note that the calculation of $p(\text{TN}|\hat{x})$ does not depend on any specific expression of ϕ . In Fig 3, we set ϕ as $\mathcal{N}(0, 1)$ only for illustration of how α impacts on $\phi_{\text{TN}}(\hat{x})$ and $\phi_{\text{FN}}(\hat{x})$.

3.2. Hard Negative Mining

We next consider the hard principle for the design of sampling distribution. We note that the posterior estimator of Eq. (17) mainly targets on the problem of false negative debiasing. It is worth emphasizing that the posterior estimation $p(\text{TN}|\hat{x})$ is determined by τ as prior class probability and relative position of observation $\Phi_n(\hat{x})$ as likelihood, with the mixture coefficient α as a correction indicator for the performance of an encoder f . Yet $p(\text{TN}|\hat{x})$ is un-affected by

specific expressions of ϕ . With such properties, it is much easier to combine the ingredient of hardness to the desired sampling distribution.

We adopt the von Mises–Fisher distribution (Mardia et al., 2000; Robinson et al., 2021) to describe the unlabeled negative samples x^- that are embedded around the anchor embedding $f(x)$ with the unnormalized density $p(x^-) \propto e^{\beta f(x)^T f(x^-)}$. As such, the density of \hat{x} conditioned on hardness is up-weighted by:

$$p(\hat{x}|\text{HARD}) \propto \phi(\hat{x})\hat{x}^\beta, \quad (19)$$

where β is the *concentration parameter* that controls the concentration degree of unlabeled samples around an anchor. So the desired sampling distribution for drawing $\{x_i^-\}_{i=1}^N$ conditioning on both true principle and hard principle can be derived as:

$$\begin{aligned} \psi(\hat{x}; \alpha, \beta) &\triangleq p(\hat{x}|\text{TN}, \text{HARD}) \\ &\propto p(\hat{x}, \text{TN}|\text{HARD}) \end{aligned} \quad (20)$$

$$\begin{aligned} &= p(\text{TN}|\hat{x}, \text{HARD})p(\hat{x}|\text{HARD}) \\ &= p(\text{TN}|\hat{x})p(\hat{x}|\text{HARD}) \end{aligned} \quad (21)$$

$$= p(\text{TN}|\hat{x}) \cdot \phi(\hat{x})\hat{x}^\beta \quad (22)$$

The symbol \propto in Eq. (20) is obtained by omitting $p(\text{TN}|\text{HARD})$ as the normalization constant, and the symbol equality in Eq. (21) is obtained using the property of posterior estimation: The assumption of von Mises–Fisher conditioned on different hard level HARD in Eq. (19) is essentially taking a specific expression of ϕ , which is independent of the posterior estimator $p(\text{TN}|\hat{x})$. Intuitively, different hard level controls different concentration degree of observations, but do not change the relative position of observations $\Phi_n(\hat{x})$ in Eq. (17).

3.3. Monte Carlo Importance Sampling

With the desired sampling distribution ψ , we can approximate the expectation over hard and true samples using classic Monte-Carlo importance sampling (Hesterberg, 1988; Bengio & Senécal, 2008):

$$\begin{aligned} \mathbb{E}_{\hat{x} \sim \psi} \hat{x} &= \int_0^{+\infty} \hat{x} \frac{\psi(\hat{x})}{\phi(\hat{x})} \phi(\hat{x}) d\hat{x} \\ &= \mathbb{E}_{\hat{x} \sim \phi} \hat{x} \frac{\psi(\hat{x})}{\phi(\hat{x})} \\ &\simeq \frac{1}{N} \sum_{i=1}^N \omega_i \hat{x}_i \end{aligned} \quad (23)$$

where ω_i is the density ratio between ψ and ϕ , which can be calculated by:

$$\begin{aligned}\omega_i(\hat{x}_i; \alpha, \beta) &= \frac{\psi(\hat{x}_i)/Z_\psi}{\phi(\hat{x}_i)} \\ &= \frac{p(\text{TN}|\hat{x}_i) \cdot \phi(\hat{x}_i)\hat{x}_i^\beta/Z_\psi}{\phi(\hat{x}_i)} \\ &= \frac{p(\text{TN}|\hat{x}_i) \cdot \hat{x}_i^\beta}{Z_\psi}.\end{aligned}\quad (24)$$

Z_ψ is the partition function of ψ since it is unnormalized, which admits the following empirical estimate:

$$\begin{aligned}Z_\psi &= \int_0^\infty \psi(\hat{x}; \alpha, \beta) d\hat{x} \\ &= \int_0^\infty p(\text{TN}|\hat{x})\hat{x}^\beta \cdot \phi(\hat{x}) d\hat{x} \\ &= \mathbb{E}_{\hat{x} \sim \phi} p(\text{TN}|\hat{x})\hat{x}^\beta \\ &\simeq \frac{1}{N} \sum_{i=1}^N p(\text{TN}|\hat{x}_i)\hat{x}_i^\beta\end{aligned}\quad (25)$$

Inserting Eq. (25) into Eq. (24), we obtain:

$$\omega_i(\hat{x}_i; \alpha, \beta) = \frac{p(\text{TN}|\hat{x}_i) \cdot \hat{x}_i^\beta}{\frac{1}{N} \sum_{i=1}^N p(\text{TN}|\hat{x}_i) \cdot \hat{x}_i^\beta}.\quad (26)$$

The quantities $\omega_i(\hat{x}_i; \alpha, \beta)$ is a function of \hat{x}_i , called as *importance weights* in this paper. They are used to correct the bias due to sampling $x^- \sim p_d$, with non-strict sense of location parameter α conditioning on the true negative principle and concentration parameter β conditioning on the hard negative principle. Intuitively, $\omega_i(\hat{x}_i; \alpha, \beta)$ down-weights a false negative sample by the $p(\text{TN}|\hat{x}_i)$ term; While it up-weights a hard negative sample by the \hat{x}_i^β term.

So far we have finished the derivations of ω computation for our BCL contrastive loss as defined in Eq. (1). It is important to state that we introduce the calculable empirical distribution function $\Phi_n(\hat{x})$ as the likelihood as well as the α as the encoder correction factor to compute the posterior estimator $p(\text{TN}|\hat{x}) = \tau^-$. In particular, for a very poor encoder with $\alpha = 1/2$, the posterior estimator reduces to $p(\text{TN}|\hat{x}) = \tau^-$, indicating that the encoder does not provide any useful information for re-weighting \hat{x}_i^- . Next we relate the proposed loss \mathcal{L}_{BCL} to \mathcal{L}_{SUP} , and show \mathcal{L}_{BCL} leads to a consistent estimation.

Lemma 3.2 (Asymptotic Unbiased Estimation). *For any encoder f and as $N \rightarrow \infty$ we observe $\mathcal{L}_{\text{SUP}} \rightarrow \mathcal{L}_{\text{BCL}}$.*

Proof. See Appendix C.2 \square

Complexity: The steps for \mathcal{L}_{BCL} computation in one training epoch have been summarized in Section 1. Compared

with the InfoNCE loss $\mathcal{L}_{\text{BIASED}}$, the additional computation complexity comes from first calculating the empirical distribution function $\Phi_n(\hat{x})$ in the order of $\mathcal{O}(N)$, which can be neglected as it is far smaller than encoding a sample.

4. Numerical Experiments

4.1. Experiment Objective

A contrastive loss is used in combination with an encoder, like a neural network, to learn representations for a downstream task, like image classification. However, in practice tasks and encoders are often with too many choices. As such, we argue only using task performance may not be enough for evaluating a contrastive loss. Instead, we propose and design the following numerical experiments to compare contrastive losses. The objective is to compare the difference between a unsupervised and a supervised contrastive loss.

Recall that the core operation of a self-supervised contrastive loss is to estimate the expectation of \hat{x}_i (Chuang et al., 2020), where $x_i \in \text{TN}$, $\hat{x}_i \triangleq e^{f(x)^T f(x_i)}$, to approximate the supervised loss \mathcal{L}_{SUP} using N randomly selected unlabeled samples x_i . For the supervised loss \mathcal{L}_{SUP} , we define the mean of true negative samples' observations by

$$\theta_{\text{SUP}} = \frac{\sum_{i=1}^N \mathbb{I}(x_i) \cdot \hat{x}_i}{\sum_{i=1}^N \mathbb{I}(x_i)},\quad (27)$$

where $\mathbb{I}(x_i)$ is the indicator function, $\mathbb{I}(x_i) = 1$ if $x_i \in \text{TN}$; Otherwise, $\mathbb{I}(x_i) = 0$, since the expectation is replaced by empirical estimates in practice (Oord et al., 2018; Chuang et al., 2020; Chen et al., 2020a). For the proposed self-supervised loss \mathcal{L}_{BCL} , we define the BCL estimator by

$$\hat{\theta}_{\text{BCL}} = \frac{1}{N} \sum_{i=1}^N \omega_i \cdot \hat{x}_i.\quad (28)$$

The empirical counterpart of a unsupervised loss \mathcal{L}_{BCL} equals to supervised loss \mathcal{L}_{SUP} , as if $\hat{\theta}_{\text{BCL}} = \hat{\theta}_{\text{SUP}}$. We compare with the following two estimators: the $\hat{\theta}_{\text{BIASED}}$ by (Oord et al., 2018) and θ_{DCL} by (Chuang et al., 2020).

$$\hat{\theta}_{\text{BIASED}} = \frac{1}{N} \sum_{i=1}^N \hat{x}_i\quad (29)$$

$$\hat{\theta}_{\text{DCL}} = \frac{1}{N\tau^-} \left(\sum_{i=1}^N \hat{x}_i - N\tau^+ \cdot \frac{\sum_{j=1}^K \hat{x}_j^+}{K} \right)\quad (30)$$

Eq. (30) can be understood as the summation of TN samples' observations divided by the number of TN samples $N\tau^-$. Specifically, $N\tau^+$ is the number of FN samples, and $\sum_{j=1}^K \hat{x}_j^+/K$ is the mean value of K FN samples. So the second term inside the parenthesis corresponds to the summation of FN samples' observations among N samples; While subtracting it from $\sum_{i=1}^N \hat{x}_i$ corresponds to the summation of TN samples among N randomly selected samples.

4.2. Experiment Design

We design a stochastic process framework to simulate \hat{x} , which depicts the numerical generative process of observation \hat{x} . In short, an observation \hat{x} is realized in the following sample function space.

Definition 4.1 (Sample Function Space). Consider a function of observation $X(x, e)$ of two variables defined on $\mathcal{X} \times \Omega$. For an anchor $x \in \mathcal{X}$, $X(x, e)$ is a random variable on a probability space (Ω, \mathcal{F}, P) related to the randomly selected unlabeled samples x_i ; For a fixed $e \in \Omega$, $X(x, e)$ is a sample function related to different anchors. We call $\{X(x, e) : x \in \mathcal{X}, e \in \Omega\}$ a sample function space.

In the sample function space, an anchor x determines the parameter of (Ω, \mathcal{F}, P) , where P is the anchor-specific proposal distribution ϕ . As ϕ is not required to be identical for different anchors, it simulates the situation that different anchors may result in different distributions of observations. Note that M anchors correspond to M sequences of random variables, each sequence with different parameters. For an anchor x , a brief description of generating an observation \hat{x} is as follows:

- (i) Select a class label according to the class probability τ^+ , indicating that the observation comes from FN with probability τ^+ , or comes from TN with probability τ^- .
- (ii) Generate an observation \hat{x} from the class conditional density ϕ_{FN} (or ϕ_{TN}), dependent on the anchor-specific ϕ , and location parameter α .
- (iii) Map \hat{x} to $\exp(\hat{x}/t)$ as the final observation.

An illustrative example is presented in Fig 7 of Appendix. Repeat the process to generate N observations for one anchor and repeat it for M anchors, we obtain $\{\exp(\hat{x}_{mi}/t) : m = 1, \dots, M, i = 1, \dots, N\}$ corresponding to an empirical observation from the sample function space $\{X(x, e) : x \in \mathcal{X}, e \in \Omega\}$. The complete stochastic process depiction of observations is presented in Algorithm 1 of Appendix B.1.

Note that in (ii), even if we set ϕ as a simple distribution, the corresponding class conditional density ϕ_{FN} (or ϕ_{TN}) is no longer a simple distribution. It is difficult to directly draw observations from ϕ_{FN} (or ϕ_{TN}). In this paper, we generate the observations from ϕ_{FN} (or ϕ_{TN}) using the accept-reject sampling (Casella et al., 2004) technique (see Algorithm 2 and 3 of Appendix B.1 for implementation details).

Note that in (iii), although the corresponding density expression of $\exp(\hat{x}/t)$ is extremely complicated, $\hat{x} \rightarrow \exp(\hat{x}/t)$ is a strictly monotonic transformation, making the empirical distribution function remains the same: $\Phi_n(\hat{x}) = \Phi_n(\exp(\hat{x}/t))$.

Fig 4 plots the empirical distribution of $\exp(\hat{x}/t)$ according to the above generative process, which corresponds to the

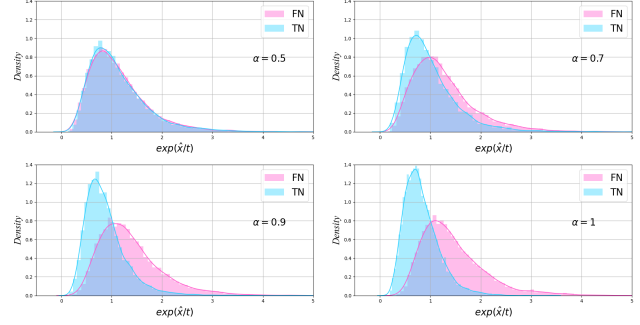


Figure 4. Empirical distribution of $\exp(\hat{x}/t)$ with different α settings. The density is fitted by using Gaussian kernel.

distribution depicted in Fig 3, where we set $t = 2$, $M = 1$ and $N = 20000$. We note that the empirical distributions in Fig 4 exhibits similar structures to those by using real-world datasets as reported in (Robinson et al., 2021; Xia et al., 2022), indicating the effectiveness of the proposed stochastic process depiction framework for simulating \hat{x} .

4.3. Experiment Results

We evaluate the quality of estimators in terms of *mean squared error* (MSE). For M anchors, we calculate $\text{MSE } \hat{\theta}_{\text{BCL}} = \frac{1}{M} \sum_{m=1}^M (\hat{\theta}_{\text{BCL},m} - \theta_{\text{SUP},m})^2$. Fig. 5 compares the MSE of different estimators against different parameters. It can be observed that the estimator $\hat{\theta}_{\text{BCL}}$ is superior than the other two estimators in terms of lower MSE with different parameter settings. We refer to Appendix B.1 for detailed settings of our numerical experiments. A particular notice here is that we set $\beta = 0$ in the ω computation, as β is designed in consideration of the requirements of downstream task that pushing TN samples further apart, other than statistical quality of $\hat{\theta}_{\text{BCL}}$.

5. Real Dataset Experiments

Thanks to the SimCLR (Chen et al., 2020a), DCL (Chuang et al., 2020) and HCL (Robinson et al., 2021) for providing the experiment framework and source codes. We conduct the real dataset experiments with the same settings as theirs for two vision tasks using the CIFAR10 (Krizhevsky & Hinton, 2009) and STL10 (Adam et al., 2011) datasets (Detailed settings are also provided in Appendix B.2).

- SimCLR (Chen et al., 2020a): It provides the experiment framework for all competitors, which comprises of a stochastic data augmentation module, the ResNet-50 as an encoder, neural network projection head. It uses the contrastive loss $\mathcal{L}_{\text{BIASED}}$.
- DCL (Chuang et al., 2020): It mainly considers the

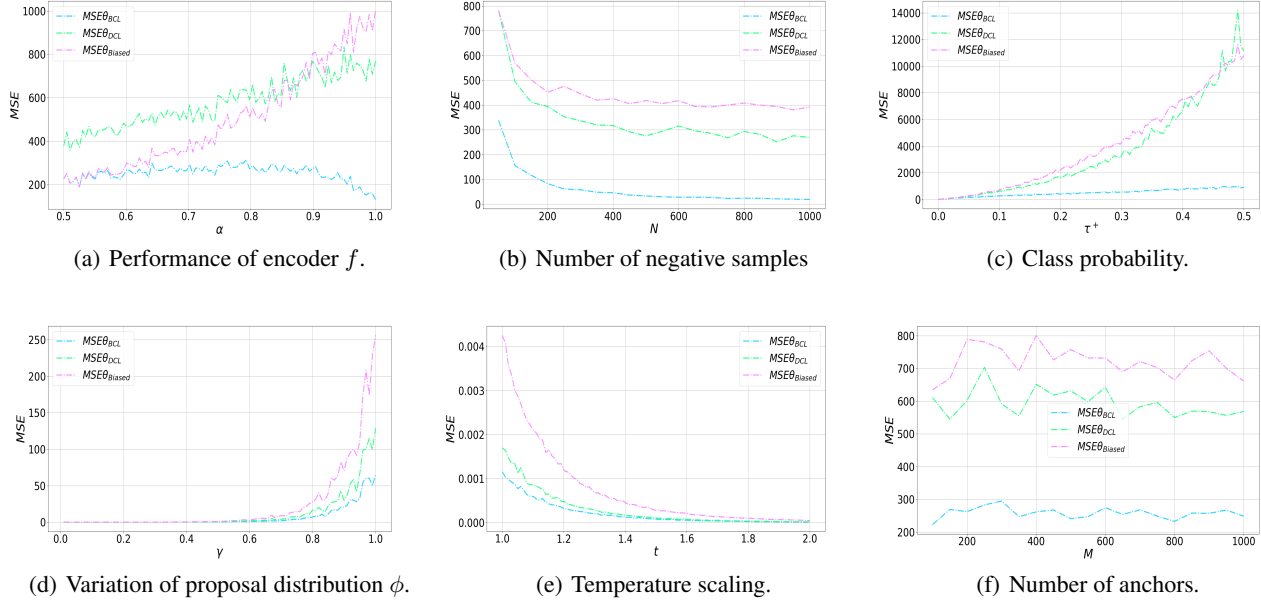


Figure 5. MSE of different estimators with various parameter settings.

false negative debiasing task and uses the estimator Eq. (30) to replace the second term in the denominator of $\mathcal{L}_{\text{BIASED}}$.

- HCL (Robinson et al., 2021): Following the DCL debiasing framework, it also takes into consideration of hard negative mining by up-weighting each randomly selected sample as follows.

$$\omega_i^{\text{HCL}} = \frac{\hat{x}_i^\beta}{\frac{1}{N} \sum_{j=1}^N \hat{x}_j^\beta}. \quad (31)$$

which is capable of independently performing false negative debiasing task and hard negative mining task. In addition, the BCL utilizes sample information to down-weight the relatively close negative samples in the embedding space (those having larger $\Phi_n(\hat{x})$, smaller $p(\text{TN}|\hat{x})$ and higher confidence of being FN). With the same hard level of HCL, the BCL increases model’s tolerance to FN samples.

6. Conclusion

This paper has proposed a BCL loss for self-supervised contrastive learning, which uses the importance sampling for correcting the bias of using random negative samples drawn from un-labeled data. The key idea is to design the desired sampling distribution under the Bayesian framework. The prominent advantage lies in that the desired sampling distribution is a parametric structure, with a location parameter correspond to encoder’s macro-AUC metric for debiasing false negative, and concentration parameter correspond to embeddings concentration degree for mining hard negative, respectively. In our future work, we shall investigate using ψ for guiding explicit negative sampling (Xu et al., 2022), and exploiting the optimal tradeoff between the false negative debiasing and hard negative mining.

Table 1. Classification accuracy on CIFAR10 and STL10.

Dataset	Methods	Negative Sample Size N				
		N=30	N=62	N=126	N=254	N=510
CIFAR10	SimCLR	80.21	84.82	87.58	89.87	91.12
	DCL	82.41	87.60	90.38	91.36	91.78
	HCL	83.42	88.45	90.53	91.57	91.62
	BCL	83.61	88.56	90.83	91.87	92.18
STL10	SimCLR	61.20	71.69	74.36	77.33	80.20
	DCL	63.91	71.48	76.69	81.48	84.23
	HCL	67.24	73.38	79.44	83.82	86.32
	BCL	67.45	73.36	80.23	84.68	86.51

Table 1 validates the effectiveness of the BCL with some performance improvements over the competitors. We next discuss the the advantage of our BCL loss. The debiasing mechanism of DCL and HCL includes a correction term in the denominator, which equally modifies the gradient magnitude for all random samples. While the BCL modifies the gradient magnitude for each random sample individually,

References

- Adam, C., Andrew, N., and Honglak, L. An analysis of single-layer networks in unsupervised feature learning. In *Proceedings of the fourteenth international conference on artificial intelligence and statistics*, pp. 215–223, 2011.
- Alec, R., Karthik, N., Tim, S., and Ilya, S. Improving language understanding by generative pre-training. 2018.
- Alec, R., Jeffrey, W., Rewon, C., David, L., Dario, A., and Ilya, S. Language models are unsupervised multitask learners. 2019.
- Bachman, P., Hjelm, R. D., and Buchwalter, W. Learning representations by maximizing mutual information across views. 2019.
- Belghazi, M. I., Baratin, A., Rajeswar, S., Ozair, S., Bengio, Y., Courville, A., and Hjelm, R. D. Mine: mutual information neural estimation. In *ICML*, 2018.
- Bengio, Y. and Senécal, J.-S. Adaptive importance sampling to accelerate training of a neural probabilistic language model. *IEEE Transactions on Neural Networks*, 19(4): 713–722, 2008.
- Casella, G., Robert, C. P., and Wells, M. T. Generalized accept-reject sampling schemes. *Lecture Notes-Monograph Series*, pp. 342–347, 2004.
- Chen, T., Kornblith, S., Norouzi, M., and Hinton, G. A simple framework for contrastive learning of visual representations. In *ICML*, pp. 1597–1607, 2020a.
- Chen, T., Kornblith, S., Swersky, K., Norouzi, M., and Hinton, G. E. Big self-supervised models are strong semi-supervised learners. *NeurIPS*, 33:22243–22255, 2020b.
- Chen, X., Fan, H., Girshick, R., and He, K. Improved baselines with momentum contrastive learning. *arXiv preprint arXiv:2003.04297*, 2020c.
- Chopra, S., Hadsell, R., and LeCun, Y. Learning a similarity metric discriminatively, with application to face verification. In *CVPR*, pp. 539–546, 2005.
- Chuang, C.-Y., Robinson, J., Lin, Y.-C., Torralba, A., and Jegelka, S. Debaised contrastive learning. In *NeurIPS*, pp. 8765–8775, 2020.
- David, H. A. and Nagaraja, H. N. *Order statistics*. 2004. ISBN 9780471654018.
- Dempster, A. P., Laird, N. M., and Rubin, D. B. Maximum likelihood from incomplete data via the em algorithm. *Journal of the Royal Statistical Society: Series B (Methodological)*, 39(1):1–22, 1977.
- Devlin, J., Chang, M.-W., Lee, K., and Toutanova, K. Bert: Pre-training of deep bidirectional transformers for language understanding. *arXiv preprint arXiv:1810.04805*, 2018.
- DeVries, T. and Taylor, G. W. Improved regularization of convolutional neural networks with cutout. *arXiv preprint arXiv:1708.04552*, 2017.
- Diederik, P. and Jimmy, B. Adam: A method for stochastic optimization. In *ICLR*, 2015.
- Dosovitskiy, A., Springenberg, J. T., Riedmiller, M., and Brox, T. Discriminative unsupervised feature learning with convolutional neural networks. In *NeurIPS*, pp. 766–774, 2014.
- Du Plessis, M., Niu, G., and Sugiyama, M. Convex formulation for learning from positive and unlabeled data. In *International conference on machine learning*, pp. 1386–1394. PMLR, 2015.
- Du Plessis, M. C., Niu, G., and Sugiyama, M. Analysis of learning from positive and unlabeled data. In *NeurIPS*, 2014.
- Florian, S., Dmitry, K., and James, P. Facenet: A unified embedding for face recognition and clustering. In *CVPR*, pp. 815–823, 2015.
- Glivenko, V. Sulla determinazione empirica delle leggi di probabilita. *Gion. Ist. Ital. Attuari.*, 4:92–99, 1933.
- Gutmann, M. and Hyvärinen, A. Noise-contrastive estimation: A new estimation principle for unnormalized statistical models. In *Proceedings of the thirteenth international conference on artificial intelligence and statistics*, pp. 297–304, 2010.
- Gutmann, M. U. and Hyvärinen, A. Noise-contrastive estimation of unnormalized statistical models, with applications to natural image statistics. *Journal of machine learning research*, 13(2), 2012.
- Hadsell, R., Chopra, S., and LeCun, Y. Dimensionality reduction by learning an invariant mapping. In *CVPR*, pp. 1735–1742, 2006.
- He, K., Zhang, X., Ren, S., and Sun, J. Deep residual learning for image recognition. In *CVPR*, pp. 770–778, 2016.
- He, K., Fan, H., Wu, Y., Xie, S., and Girshick, R. Momentum contrast for unsupervised visual representation learning. In *CVPR*, pp. 9729–9738, 2020.
- Henaff, O. Data-efficient image recognition with contrastive predictive coding. In *ICML*, pp. 4182–4192, 2020.

- Hesterberg, T. C. *Advances in importance sampling*. Stanford University, 1988.
- Hjelm, R. D., Fedorov, A., Lavoie-Marchildon, S., Grewal, K., Bachman, P., Trischler, A., and Bengio, Y. Learning deep representations by mutual information estimation and maximization. *arXiv preprint arXiv:1808.06670*, 2018.
- Huang, J., Dong, Q., Gong, S., and Zhu, X. Unsupervised deep learning by neighbourhood discovery. In *ICML*, pp. 2849–2858, 2019.
- Hyun, Oh, S., Yu, X., Stefanie, J., and Silvio, S. Deep metric learning via lifted structured feature embedding. In *CVPR*, pp. 4004–4012, 2016.
- Jessa, B. and Jesse, D. Learning from positive and unlabeled data: a survey. *Machine Learning*, 109:719–760, 2020.
- Khosla, P., Teterwak, P., Wang, C., Sarna, A., Tian, Y., Isola, P., Maschinot, A., Liu, C., and Krishnan, D. Supervised contrastive learning. In *NeurIPS*, pp. 18661–18673, 2020.
- Kiryo, R., Niu, G., Du Plessis, M. C., and Sugiyama, M. Positive-unlabeled learning with non-negative risk estimator. In *NeurIPS*, 2017.
- Komodakis, N. and Gidaris, S. Unsupervised representation learning by predicting image rotations. In *ICLR*, 2018.
- Krizhevsky, A. and Hinton, G. Learning multiple layers of features from tiny images. 2009.
- Lajanugen, L. and Honglak, L. An efficient framework for learning sentence representations. In *ICLR*, 2018.
- Lindsay, B. *Mixture Models: Theory, Geometry and Applications*. 1995. ISBN 0-94-0600-32-3.
- Liu, X., Zhang, F., Hou, Z., Mian, L., Wang, Z., Zhang, J., and Tang, J. Self-supervised learning: Generative or contrastive. *IEEE Transactions on Knowledge and Data Engineering*, 2021.
- Mardia, K. V., Jupp, P. E., and Mardia, K. *Directional statistics*, volume 2. Wiley Online Library, 2000.
- Misra, I. and Maaten, L. v. d. Self-supervised learning of pretext-invariant representations. In *CVPR*, pp. 6707–6717, 2020.
- Oord, A. v. d., Li, Y., and Vinyals, O. Representation learning with contrastive predictive coding. *arXiv preprint arXiv:1807.03748*, 2018.
- Poole, B., Ozair, S., van den Oord, A., Alemi, A. A., and Tucker, G. On variational bounds of mutual information. In *ICML*, pp. 5171–5180, 2019.
- Robinson, J., Ching-Yao, C., Sra, S., and Jegelka, S. Contrastive learning with hard negative samples. In *ICLR*, 2021.
- Saunshi, N., Plevrakis, O., Arora, S., Khodak, M., and Khandeparkar, H. A theoretical analysis of contrastive unsupervised representation learning. In *ICML*, pp. 5628–5637, 2019.
- Szegedy, C., Liu, W., Jia, Y., Sermanet, P., Reed, S., Anguelov, D., Erhan, D., Vanhoucke, V., and Rabinovich, A. Going deeper with convolutions. In *CVPR*, pp. 1–9, 2015.
- Tian, Y., Krishnan, D., and Isola, P. Contrastive multiview coding. In *ECCV*, pp. 776–794, 2020.
- Wang, F. and Liu, H. Understanding the behaviour of contrastive loss. In *CVPR*, pp. 2495–2504, 2021.
- Wang, T. and Isola, P. Understanding contrastive representation learning through alignment and uniformity on the hypersphere. In *ICML*, pp. 9929–9939, 2020.
- Wu, Z., Xiong, Y., Yu, S. X., and Lin, D. Unsupervised feature learning via non-parametric instance discrimination. In *CVPR*, pp. 3733–3742, 2018.
- Xia, J., Wu, L., Wang, G., Chen, J., and Li, S. Z. Progl: Rethinking hard negative mining in graph contrastive learning. In *ICML*, pp. 24332–24346, 2022.
- Xu, L., Lian, J., Zhao, W. X., Gong, M., Shou, L., Jiang, D., Xie, X., and Wen, J.-R. Negative sampling for contrastive representation learning: A review. *arXiv preprint arXiv:2206.00212*, 2022.
- Yannis, K., Mert, Bulent, S., Noe, P., Philippe, W., and Diane, L. Hard negative mixing for contrastive learning. In *NeurIPS*, pp. 21798–21809, 2020.
- Zhuang, C., Zhai, A. L., and Yamins, D. Local aggregation for unsupervised learning of visual embeddings. In *CVPR*, pp. 6002–6012, 2019.

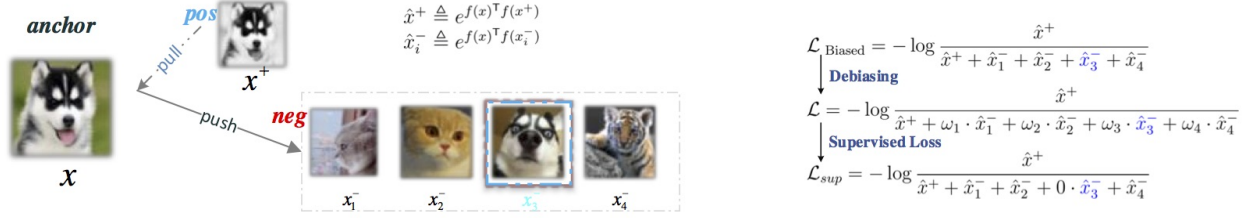


Figure 6. Illustrative example of debiased contrastive objective inspired by (Chuang et al., 2020).

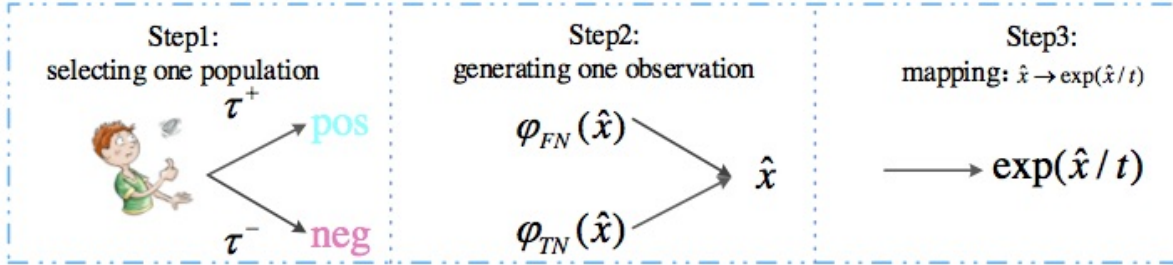


Figure 7. Generation process of observation $\exp(\hat{x}/t)$ for one anchor.

A. Related Work

Contrastive learning adopts the *learn-to-compare* paradigm (Gutmann & Hyvärinen, 2010) that discriminates the observed data from noise data to relieve the model from reconstructing pixel-level information of data (Oord et al., 2018). Although the representation encoder f and similarity measure vary from task to task (Devlin et al., 2018; He et al., 2020; Dosovitskiy et al., 2014), they share an identical basic idea of contrasting similar pairs (x, x^+) and dissimilar pairs (x, x^-) to train f by optimizing a contrastive loss (Wang & Isola, 2020), such as the NCE loss (Gutmann & Hyvärinen, 2010), InfoNCE loss (Oord et al., 2018), Infomax loss (Hjelm et al., 2018), asymptotic contrastive loss (Wang & Isola, 2020) and etc. These loss functions implicitly (Oord et al., 2018) or explicitly (Hjelm et al., 2018) lower bounds the mutual information. Arora et al. (Saunshi et al., 2019) provide theoretical analysis on the generalization bound of contrastive learning for classification tasks. Remarkable successes of supervised contrastive learning have been observed for many applications in different domains (Henaff, 2020; Khosla et al., 2020), but the great limitations are from their dependent on manually labeled datasets (Liu et al., 2021).

Self-supervised contrastive learning (Chen et al., 2020a;b; He et al., 2020; Henaff, 2020; Xu et al., 2022) has been extensively researched for its advantages of learning representations without human labelers for manually labeling data, and benefits almost all types of downstream tasks (Liu et al., 2021; Bachman et al., 2019; Chen et al., 2020c; Huang et al., 2019; Wu et al., 2018; Zhuang et al., 2019). The common practice is to obtain positive sample x^+ from some semantic-invariant operation on an anchor x with heavy data augmentation (Chen et al., 2020a), like random cropping and flipping (Oord et al., 2018), image rotation (Komodakis & Gidaris, 2018), cutout (DeVries & Taylor, 2017) and color distortion (Szegedy et al., 2015); While drawing negative samples x^- simply from un-labeled data, which introduces the false negative problem, leading to incorrect encoder training. This problem is related to the classic positive-unlabeled (PU) learning (Jessa & Jesse, 2020), where the unlabeled data used as negative samples would be down-weighted appropriately (Du Plessis et al., 2015; 2014; Kiryo et al., 2017). However, existing PU estimators are not directly applicable to contrastive loss. In particular, two conflicting tasks are faced in self-supervised contrastive learning (Liu et al., 2021; Robinson et al., 2021): false negative debiasing and hard negative mining. How to estimate the probability of an unlabeled sample being a true negative sample,

Algorithm 1 Numerical experiments.

Input: location parameter α (mixtrue coffecient), temperature scaling t
Output: Observations and labels.

```

for anchor  $m = 1, 2, \dots, M$  do
    \ \ choose an anchor-specific distribution  $\phi$ .
    Random select  $[a, b] \subseteq [-1/t^2, 1/t^2]$ 
    Set  $\phi \sim U(a, b)$ 
    for negative  $j = 1, 2, \dots, N$  do
        \ \ step1:selecting one population
         $p = \text{random.uniform}(0,1)$ 
        if  $p \leq \tau^+$  then
            \ \ step2:generating observation from  $\phi_{\text{FN}}$ 
             $\hat{x}_j = \text{AccRejetSamplingFN}(\phi_{\text{FN}})$ 
            label = False
        else
            \ \ step2:generating observation from  $\phi_{\text{TN}}$ 
             $\hat{x}_j = \text{AccRejetSamplingTN}(\phi_{\text{TN}})$ 
            label = True
        \ \ step3:mapping
         $\hat{x}_j = \exp(\hat{x}_j/t)$ 
        collecting observation  $\hat{x}$  and label
    
```

Result: Observations and labels.

thus how to optimally trade-off the two tasks still remains unsolved.

B. Implementation details of experiments

B.1. Numerical experiments

Chosen of proposal distribution ϕ . For the convenience of controlling the observation within its theoretical minimum and maximum interval $[-1/t^2, 1/t^2]$, as well as the previous research show that contrastive loss optimizes the negative samples for uniformity asymptotically (Wang & Isola, 2020), we set ϕ as $U(a, b)$ to perform the numerical experiment, where $-1/t^2 \leq a \leq b \leq 1/t^2$ is random selected for each anchor. Specifically, the original interval was set as $a = -0.5$, $b = 0.5$, and use $\gamma \in [0, 1]$ to control the maximum sliding amplitude from the original interval.

Implementation of accept-reject sampling. The objective is to generate sample \hat{x} from class conditional density $\phi_{\text{TN}}(\hat{x})$, i.e., $\hat{x} \sim \phi_{\text{TN}}(\hat{x})$. The basic idea is to generate a sample \hat{x} from proposal distribution ϕ , and accept it with acceptance probability p_{TN} . To calculate the acceptance probability p_{TN} , we first write $\phi_{\text{TN}}(\hat{x})$ as a function of proposal distribution $\phi(\hat{x})$

$$\begin{aligned}
 \phi_{\text{TN}}(\hat{x}) &= \alpha\phi_{(1)}(\hat{x}) + (1 - \alpha)\phi_{(2)}(\hat{x}) \\
 &= [2\alpha + (2 - 4\alpha)\Phi(\hat{x})]\phi(\hat{x}),
 \end{aligned}$$

where $\Phi(\hat{x})$ is the c.d.f. of proposal distribution $\phi(\hat{x})$. Next we find a minimum c that satisfies the following inequality:

$$c \cdot \phi(\hat{x}) \geq \phi_{\text{TN}}(\hat{x}),$$

that is

$$c \cdot \phi(\hat{x}) \geq [2\alpha + (2 - 4\alpha)\Phi(\hat{x})]\phi(\hat{x}).$$

So the minimal of c is attained

$$\begin{aligned}
 c &= \min[2\alpha + (2 - 4\alpha)\Phi(\hat{x}), \Phi(\hat{x}) \in [0, 1] \\
 &= 2\alpha,
 \end{aligned}$$

when $\Phi(\hat{x}) = 0$ since $2 - 4\alpha \leq 0$. So the acceptance probability is

$$\begin{aligned} p_{\text{TN}} &= \frac{\phi_{\text{TN}}(\hat{x})}{c \cdot \phi(\hat{x})} \\ &= [\alpha + (1 - 2\alpha) \cdot \Phi(\hat{x})] / \alpha \end{aligned}$$

An observation \hat{x} generated from proposal distribution $\phi(\hat{x})$ is accepted with probability p_{TN} , formulates the empirical observations $\hat{x} \sim \phi_{\text{TN}}(\hat{x})$ as described in Algorithm 2.

Algorithm 2 AccRejetSamplingTN(ϕ_{TN}).

Input: location parameter α , proposal distrition ϕ

Output: samples $\hat{x} \sim \phi_{\text{TN}}$.

```

 $\hat{x}_j$  = generate observation  $\hat{x}_j$  from  $\phi$ 
cdf =  $\int_{-\infty}^{\hat{x}_j} \phi(t)dt$ 
u = random.uniform(0, 1)
while  $u > [\alpha + (1 - 2\alpha) \cdot \text{cdf}] / \alpha$  do
     $\hat{x}_j$  = generate observation  $\hat{x}_j$  from  $\phi$ 
    cdf =  $\int_{-\infty}^{\hat{x}_j} \phi(t)dt$ 
    u = random.uniform(0, 1)
```

Result: \hat{x}_j

Likewise, the acceptance probability for ϕ_{FN}

$$p_{\text{FN}} = [1 - \alpha + (2\alpha - 1) \cdot \Phi(\hat{x})] / \alpha$$

can be calculated in the similar way. An observation \hat{x} from proposal distribution $\phi(\hat{x})$ is accepted with probability p_{FN} , formulates the empirical observations $\hat{x} \sim \phi_{\text{FN}}(\hat{x})$ as described in Algorithm 3.

Algorithm 3 AccRejetSamplingFN(ϕ_{FN}).

Input: location parameter α , proposal distrition ϕ

Output: samples $\hat{x} \sim \phi_{\text{FN}}$.

```

 $\hat{x}_j$  = generate observation  $\hat{x}_j$  from  $\phi$ 
cdf =  $\int_{-\infty}^{\hat{x}_j} \phi(t)dt$ 
u = random.uniform(0, 1)
while  $u > [1 - \alpha + (2\alpha - 1) \cdot \text{cdf}] / \alpha$  do
     $\hat{x}_j$  = generate observation  $\hat{x}_j$  from  $\phi$ 
    cdf =  $\int_{-\infty}^{\hat{x}_j} \phi(t)dt$ 
    u = random.uniform(0, 1)
```

Result: \hat{x}_j

Parameter Settings. For baseline estimator $\hat{\theta}_{\text{DCL}}$ in Eq (30), the number of positive samples K is fixed as 10. We start from fixing the parameters as: $\alpha = 0.9$, $\beta = 0.9$, $\gamma = 0.1$, $\tau^+ = 0.1$, temperature scaling $t = 0.5$, number of anchors $M = 1e3$, and number of negative samples $N = 64$ to investigate the performance of different estimators under different parameters settings.

Mean values. Aside from MSE , we report the mean values of the estimators $\hat{\theta}$. Our primary concern is whether the chosen of proposal distribution ϕ or encoder f affects the consistency of estimators. Fig 8(a) shows the influence of different variation of anchor-specific proposal distribution ϕ on mean values of estimators. Fig 8(b) shows the influence of encoder's performance on mean values of estimators. It can be seen that the mean value of $\hat{\theta}_{\text{BCL}}$, $\hat{\theta}_{\text{DCL}}$ and θ sequences are very close, which guaranteed by Chebyshev law of large numbers, namely $\lim_{M \rightarrow \infty} \mathbb{P}\{|\frac{1}{M} \sum_{m=1}^M \hat{\theta}_m - \frac{1}{M} \sum_{m=1}^M \theta_m| < \epsilon\} = 1$ as $\mathbb{E} \hat{\theta}_m = \theta_m$. This conclusion is un-affected by the chosen of proposal distribution ϕ or encoder f . Aside from consistency of estimators, Fig 8(b) can be seen as a simulation of training process: a better trained encoder with higher macro-AUC embeds

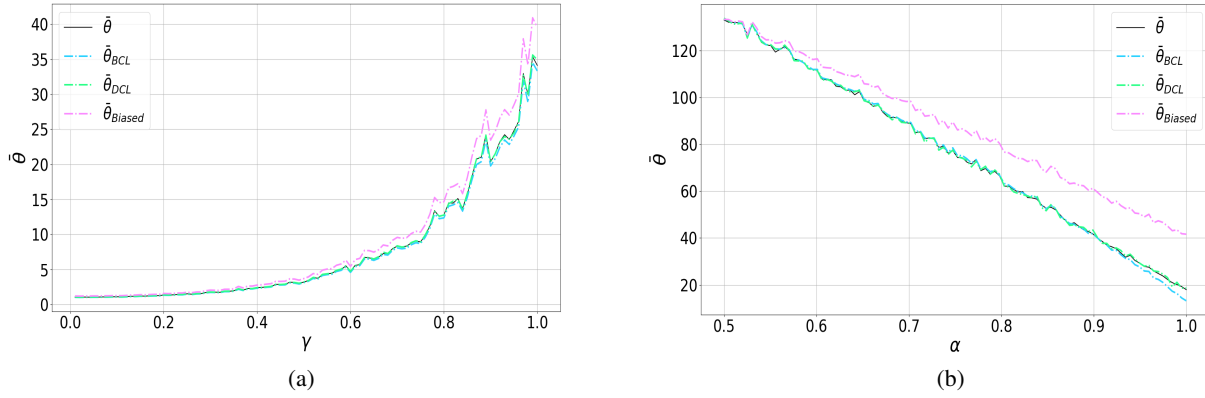


Figure 8. Mean values of estimators $\hat{\theta}$ over all anchors.

true negative samples dissimilar with anchor, while more similar to anchor for false negative samples. So we observe the decrease of $\bar{\theta}$, which corresponds to the decrease of loss values in the training process, and increase of bias $|\bar{\theta}_{BIASED} - \bar{\theta}|$ since the contained false negative samples in $\bar{\theta}_{BIASED}$ are scored higher as α increases.

B.2. Real data experiment

Experimental setup: We perform the experiments on vision tasks using CIFAR10 (Krizhevsky & Hinton, 2009) and STL10 (Adam et al., 2011) datasets. All the experimental settings are identically as DCL (Chuang et al., 2020) and HCL (Robinson et al., 2021). Specifically, we implement SimCLR (Chen et al., 2020a) with ResNet-50 (He et al., 2016) as the encoder architecture and use the Adam optimizer (Diederik & Jimmy, 2015) with learning rate 0.001. The temperature scaling and the dimension of the latent vector were set as $t = 0.5$ and $d=128$. All the models are trained for 400 epochs, and evaluated by training a linear classifier after fixing the learned embedding (Lajanugen & Honglak, 2018; Robinson et al., 2021). The source codes are available at <https://github.com/liubin06/BNS>

Location parameter α : recall that α corresponds to the encoder’s macro-AUC, we recommend the following two basic strategies for setting α :

- **Timely-adjust strategy:** setting α as empirical macro-AUC, and updated every 20 training epochs. The gradual increase of α means that the confidence level of sample information $\Phi_n(\cdot)$ increases, and a sample with relative closer embedding distance to the anchor are more likely to be a FN sample.
- **Warm-start strategy:** setting $\alpha = 0.5$ at first 300 training epochs, that is, only uses prior information τ for debiasing false negative samples to warm-up the encoder, then set $\alpha = 0.7$ at the later 100 training epochs to introduce sample information $\Phi_n(\hat{x})$ to debias false negative samples. Since the encoder has been warmed up, the sample information is more reliable.

We adopt the warm-start strategy for setting α , since the sample information is not reliable at the initial training phase, the performance gain of debiasing false negative samples is less than that of mining hard negative samples.

Concentration parameter β : it corresponds to concentration degree of embeddings. Note that contrastive loss optimizes the negative samples for uniformity asymptotically (Wang & Isola, 2020) in the training phase, which indicating the concentration degree of embeddings are gradually decreased. We therefore set β to be a decreasing function of training epoch: $\beta = 2 - 0.005 \cdot \text{epoch}$, which is also updated every 20 training epochs. $\beta = 2$ at epoch 0 indicating that BCL lays more emphasize on hard negative mining task at initial training phase, while $\beta = 0$ at epoch 400 indicating that BCL lays more emphasize on false negative debiasing task at later training phase.

C. Proofs

Proposition C.1 (Class Conditional Density). *If $\phi(\hat{x})$ is continuous density function that satisfy $\phi(\hat{x}) \geq 0$ and $\int_{-\infty}^{+\infty} \phi(\hat{x})d\hat{x} = 1$, then $\phi_{\text{TN}}(\hat{x})$ and $\phi_{\text{FN}}(\hat{x})$ are probability density functions that satisfy $\phi_{\text{TN}}(\hat{x}) \geq 0$, $\phi_{\text{FN}}(\hat{x}) \geq 0$, and $\int_{-\infty}^{+\infty} \phi_{\text{TN}}(\hat{x})d\hat{x} = 1$, $\int_{-\infty}^{+\infty} \phi_{\text{FN}}(\hat{x})d\hat{x} = 1$.*

Proof. Since $\phi(\hat{x}) \geq 0$ and $\int_{-\infty}^{+\infty} \phi(\hat{x})d\hat{x} = 1$, so

$$\begin{aligned}\phi_{\text{TN}}(\hat{x}) &= \alpha\phi_{(1)}(\hat{x}) + (1 - \alpha)\phi_{(2)}(\hat{x}) \\ &= 2\alpha\phi(\hat{x})[1 - \Phi(\hat{x})] + 2(1 - \alpha)\phi(\hat{x})\Phi(\hat{x}) \\ &\geq 0,\end{aligned}\tag{32}$$

where $\alpha \in [0.5, 1]$ and $\Phi(\hat{x}) \in [0, 1]$.

$$\begin{aligned}\int_{-\infty}^{+\infty} \phi_{\text{TN}}(\hat{x})d\hat{x} &= \int_{-\infty}^{+\infty} 2\alpha\phi(\hat{x})[1 - \Phi(\hat{x})] + 2(1 - \alpha)\phi(\hat{x})\Phi(\hat{x})d\hat{x} \\ &= 2\alpha \int_{-\infty}^{+\infty} \phi(\hat{x})[1 - \Phi(\hat{x})]d\hat{x} + 2(1 - \alpha) \int_{-\infty}^{+\infty} \phi(\hat{x})\Phi(\hat{x})d\hat{x} \\ &= 2\alpha \int_{-\infty}^{+\infty} [1 - \Phi(\hat{x})]d\Phi(\hat{x}) + 2(1 - \alpha) \int_{-\infty}^{+\infty} \Phi(\hat{x})d\Phi(\hat{x}) \\ &= 2\alpha \int_0^1 (1 - \mu)d\mu + 2(1 - \alpha) \int_0^1 \mu d\mu \\ &= [\alpha(2\mu - \mu^2) + (1 - \alpha)\mu^2] \Big|_0^1 \\ &= 1,\end{aligned}\tag{33}$$

$$\begin{aligned}&= 1,\end{aligned}\tag{34}$$

where Eq 33 is integration by substitution of $\Phi(\hat{x})$ and μ . Likewise,

$$\begin{aligned}\phi_{\text{FN}}(\hat{x}) &= \alpha\phi_{(2)}(\hat{x}) + (1 - \alpha)\phi_{(1)}(\hat{x}) \\ &= 2\alpha\phi(\hat{x})\Phi(\hat{x}) + 2(1 - \alpha)\phi(\hat{x})[1 - \Phi(\hat{x})] \\ &\geq 0,\end{aligned}\tag{35}$$

and

$$\begin{aligned}\int_{-\infty}^{+\infty} \phi_{\text{FN}}(\hat{x})d\hat{x} &= 2\alpha \int_{-\infty}^{+\infty} \phi(\hat{x})\Phi(\hat{x})d\hat{x} + 2(1 - \alpha) \int_{-\infty}^{+\infty} \phi(\hat{x})[1 - \Phi(\hat{x})]d\hat{x} \\ &= 2\alpha \int_{-\infty}^{+\infty} \Phi(\hat{x})d\Phi(\hat{x}) + 2(1 - \alpha) \int_{-\infty}^{+\infty} [1 - \Phi(\hat{x})]d\Phi(\hat{x}) \\ &= 2\alpha \int_0^1 \mu d\mu + 2(1 - \alpha) \int_0^1 (1 - \mu)d\mu \\ &= [\alpha\mu^2 + (1 - \alpha)(2\mu - \mu^2)] \Big|_0^1 \\ &= 1.\end{aligned}\tag{36}$$

□

Lemma C.2 (Asymptotic Unbiased Estimation). *For any encoder f and as $N \rightarrow \infty$, we have $\mathcal{L}_{\text{SUP}} \rightarrow \mathcal{L}_{\text{BCL}}$.*

Proof. We draw the conclusion by the Lebesgue Dominant Convergence Theorem and the properties of important sampling:

$$\begin{aligned}
 \lim_{N \rightarrow \infty} \mathcal{L}_{\text{SUP}} &= \lim_{N \rightarrow \infty} \mathbb{E}_{\substack{x \sim p_d \\ x^+ \sim p^+ \\ x^- \sim p^-}} \left[-\log \frac{e^{f(x)^T f(x^+)}}{e^{f(x)^T f(x^+)} + \sum_{i=1}^N e^{f(x)^T f(x_j^-)}} \right] \\
 &= \mathbb{E}_{\substack{x \sim p_d \\ x^+ \sim p^+ \\ x^- \sim p^-}} \lim_{N \rightarrow \infty} \left[-\log \frac{e^{f(x)^T f(x^+)}}{e^{f(x)^T f(x^+)} + \sum_{i=1}^N e^{f(x)^T f(x_j^-)}} \right] \\
 &= \mathbb{E}_{\substack{x \sim p_d \\ x^+ \sim p^+}} \lim_{N \rightarrow \infty} \left[-\log \frac{e^{f(x)^T f(x^+)}}{e^{f(x)^T f(x^+)} + N \mathbb{E}_{x^- \sim p^-} e^{f(x)^T f(x_j^-)}} \right] \\
 &= \mathbb{E}_{\substack{x \sim p_d \\ x^+ \sim p^+}} \lim_{N \rightarrow \infty} \left[-\log \frac{e^{f(x)^T f(x^+)}}{e^{f(x)^T f(x^+)} + N \cdot \int_0^{+\infty} \hat{x} \psi(\hat{x}) d\hat{x}} \right] \\
 &= \mathbb{E}_{\substack{x \sim p_d \\ x^+ \sim p^+}} \lim_{N \rightarrow \infty} \left[-\log \frac{e^{f(x)^T f(x^+)}}{e^{f(x)^T f(x^+)} + N \cdot \int_0^{+\infty} \hat{x} \frac{\psi(\hat{x})}{\phi(\hat{x})} \phi(\hat{x}) d\hat{x}} \right] \\
 &= \mathbb{E}_{\substack{x \sim p_d \\ x^+ \sim p^+}} \lim_{N \rightarrow \infty} \left[-\log \frac{e^{f(x)^T f(x^+)}}{e^{f(x)^T f(x^+)} + N \cdot \mathbb{E}_{\hat{x} \sim \phi(\hat{x})} \omega \hat{x}} \right] \\
 &= \mathbb{E}_{\substack{x \sim p_d \\ x^+ \sim p^+}} \lim_{N \rightarrow \infty} \left[-\log \frac{e^{f(x)^T f(x^+)}}{e^{f(x)^T f(x^+)} + N \cdot \mathbb{E}_{\hat{x} \sim \phi(\hat{x})} \omega \hat{x}} \right] \\
 &= \mathbb{E}_{\substack{x \sim p_d \\ x^+ \sim p^+ \\ x^- \sim p_d}} \left[-\log \frac{e^{f(x)^T f(x^+)}}{e^{f(x)^T f(x^+)} + \sum_{i=1}^N \omega_i \hat{x}_i} \right] \\
 &= \mathcal{L}_{\text{BCL}}
 \end{aligned} \tag{37}$$

□